J Arid Land (2024) 16(11): 1522–1540
doi: 10.1007/s40333-024-0033-z; CSTR: 32276.14.JAL.0240033z

Science Press Springer-Verlag

Spatiotemporal patterns and driving factors of soil protection in the wind-water erosion area of Chinese Loess Plateau

LI Qing[1,2], LI Dan[2], WANG Sheng[2*], WANG Jinfeng[2], WANG Rende[1], FU Gang[1], YUAN Yixiao[1], ZHENG Zhenhua[1]

[1] Institute of Geographical Sciences, Hebei Academy of Sciences, Hebei Technology Innovation Center for Geographic Information Application, Shijiazhuang 050011, China;
[2] School of Geographical Science, Shanxi Normal University, Taiyuan 030031, China

Abstract: As one of typical areas in the world, northern Chinese Loess Plateau experiences serious wind-water erosion, which leads to widespread land degradation. During the past decades, an ecological engineering was implemented to reduce soil erosion and improve soil protection in this area. Thus, it is necessary to recognize the basic characteristics of soil protection for sustainable prevention and wind-water erosion control in the later stage. In this study, national wind erosion survey model and revised universal soil loss equation were used to analyze the spatiotemporal evolution and driving forces of soil protection in the wind-water erosion area of Chinese Loess Plateau during 2000–2020. Results revealed that: (1) during 2000–2020, total amount of soil protection reached up to 15.47×10^8 t, which was realized mainly through water and soil conservation, accounting for 63.20% of the total; (2) soil protection was improved, with increases in both soil protection amount and soil retention rate. The amounts of wind erosion reduction showed a decrease trend, whereas the retention rate of wind erosion reduction showed an increase trend. Both water erosion reduction amount and retention rate showed increasing trends; and (3) the combined effects of climate change and human activities were responsible for the improvement of soil protection in the wind-water erosion area of Chinese Loess Plateau. The findings revealed the spatiotemporal patterns and driving forces of soil protection, and proposed strategies for future soil protection planning in Chinese Loess Plateau, which might provide valuable references for soil erosion control in other wind-water erosion areas of the world.

Keywords: soil protection; driving force; trade-off; synergy; wind-water erosion; Loess Plateau

Citation: LI Qing, LI Dan, WANG Sheng, WANG Jinfeng, WANG Rende, FU Gang, YUAN Yixiao, ZHENG Zhenhua. 2024. Spatiotemporal patterns and driving factors of soil protection in the wind-water erosion area of Chinese Loess Plateau. Journal of Arid Land, 16(11): 1522–1540. https://doi.org/10.1007/s40333-024-0033-z; https://cstr.cn/32276.14.JAL.0240033z

1 Introduction

The report of the United Nations Convention to Combat Desertification (UNCCD) states that up to 40.00% of land globally has deteriorated (UNCCD, 2022), and about 85.00% of land degradation is associated with soil erosion (Oldeman et al., 1990). Soil erosion not only affects local soil fertility and land productivity, but also increases the danger of pollution and disasters in local and surrounding areas (Cerretelli et al., 2023). Under the influence of natural environment and human activities, Chinese Loess Plateau is among the most severe soil erosion worldwide (Li

*Corresponding author: WANG Sheng (E-mail: wangsheng@sxnu.edu.cn)
Received 2024-01-22; revised 2024-08-07; accepted 2024-09-25

and Gao, 2011; Xi et al., 2017). In northern and western Loess Plateau, due to frequently strong winds in spring and heavy rainfall in summer, wind erosivity and rainfall erosivity are strong (Shen et al., 2018; Jiang et al., 2019, Cui et al., 2020; Wang et al., 2023a). Therefore, a typical wind-water erosion area with high erosion intensity was developed (Li et al., 2022). Soil protection is urgent in this area, which is essential for regional environmental sustainability and socio-economic development.

Soil protection represents the ability of vegetation to reduce water and wind erosion. Quantitative assessment can be carried out by two indicators, i.e., water erosion reduction (assessing soil and water conservation) and wind erosion reduction (assessing windbreak and sand fixation) (Wang et al., 2023c). Soil and water conservation in the Loess Plateau has received extensive attention. Related studies cover the distribution, mechanism, driving factors, and control measures (Shi and Shao, 2000; Tang et al., 2015; Xi et al., 2017; Xia et al., 2017; Jin et al., 2021; Li et al., 2022; Mu et al., 2022; Wen and Zhen, 2023; Wu et al., 2023; Zhu et al., 2023). Recently, numerical simulation has become effective means to resolve this issue with its quantitative and convenient regional-scale calculation advantages (Jodhani et al., 2023; Zhang et al., 2023a). In the Loess Plateau, Tang et al. (2015) assessed the water erosion of Yangou watershed using the revised universal soil loss equation (RUSLE). Xi et al. (2017) analyzed the impact of land use change on water erosion from the 1980s to 2010 using soil erosion severity index (SESI). Li et al. (2022) used the RUSLE to discuss the drivers and water erosion rates from 1901 to 2016. Mu et al. (2022) used the RUSLE model to study the spatiotemporal patterns and driving forces of soil-water erosion during 1901–2016. In contrast, windbreak and sand fixation received less attention in this area. Preliminary explorations of wind erosion process (Zhou et al., 2020; Pang et al., 2022), analysis of the underlying influencing factors (Han et al., 2023), and sand fixation assessment (Song et al., 2022) in some sandy lands or deserts had been conducted.

In recent decades, several ecological projects (e.g., Three-North Shelter Forest Program, National Key of Soil and Water Conservation Projects, Gain for Green Program, Natural Forest Conservation Program, Soil and Water Conservation Plan, etc.) and soil protection measures (e.g., vegetation rehabilitation, check-dam, terracing construction, etc.) have been implemented gradually in the Loess Plateau. Through the effective implementation of these ecological measures, a notable amount of regional vegetation has been restored (Chen et al., 2023), soil erosion rate has been reduced, and regional soil protection has been improved considerably (Wang et al., 2018). Identifying the spatiotemporal patterns and driving factors of soil protection are essential to evaluate the effectiveness of projects and measures. The amount of soil and water conservation in the wind-water erosion area of the Loess Plateau showed an increasing trend in recent decades. Land use changes, vegetation restoration, check-dam, and terracing construction were all important driving factors for above variations (Chen et al., 2007; Fu et al., 2011; Jiang et al., 2016; Wang et al., 2018; Feng et al., 2020; Li et al., 2024). However, studies on the spatiotemporal pattern and influencing factors of windbreak and sand fixation were lacking and unsystematic in the wind-water erosion area, which hinders the in-depth understanding of soil protection issues (Zou et al., 2024). Meanwhile, as the area is sensitive to global climate change (Liu et al., 2022), drastic changes in climate and increasingly frequent and extreme weather events (Ren et al., 2023) on the Loess Plateau will also cause significant changes in soil erosion, posing great challenge to regional soil protection studies.

Wind-water erosion area of the Loess Plateau serves as vital ecological barrier in northern China, and the major hub for Chinese energy and chemical industries. It is also an important area for socioeconomic development and ecological security. Comprehensive understanding of the spatiotemporal evolution characteristics and driving forces of regional soil protection is the basis for realization of regional ecological protection and high-quality economic growth. In this study, the modelling and spatial analysis were applied to: (1) examine the spatiotemporal evolution characteristics of soil protection in the wind-water erosion area of the Loess Plateau during 2000–2020; (2) analyze the effects of human activities and climatic variability on soil protection, and investigate the trade-off and synergy under different soil protection measures; and (3) put

forward the proposal of regional soil erosion prevention and control for wind-water erosion area.

2 Materials and methods

2.1 Study area

The Chinese Loess Plateau (34°15′N–41°16′N, 102°23′E–114°33′E; Fig. 1) covers Shanxi and Shaanxi provinces, and Inner Mongolia and Ningxia Hui autonomous regions (Shen et al., 2018). There are three types of soil erosion on the plateau, i.e., water erosion, wind erosion, and freeze-thaw erosion. The wind-water erosion area is distributed in the northern and western Loess Plateau, which is located in the transition zone between inland arid and East Asian monsoon climate areas. The inter- and intra-annual variability of regional precipitation is substantial. Mean annual precipitation spans from 131 to 593 mm. Within a year, the maximum and minimum precipitation can differ by magnitudes of 2–7 times. The precipitation during June–September accounts for >60.00% of the annual total, and it falls mainly in heavy rainfall events (Lu et al., 2022). Strong and gusty winds occur in spring, with an average wind speed of 1.2–2.7 m/s. In the wind-water erosion area of the Loess Plateau, the average vegetation coverage is only 19.23%. Soils predominantly consist of loess and sandy soil, with a loose soil structure that is prone to erosion. According to land use data from 2020, grassland accounts for 61.78% of the total area, and cultivated land and desert accounts for 26.30% and 6.90%, respectively. The unique natural conditions of the area lead to a fragile ecological environment with interleaved wind erosion and water erosion, representative of the center of high erosion modulus and strong sediment content in China.

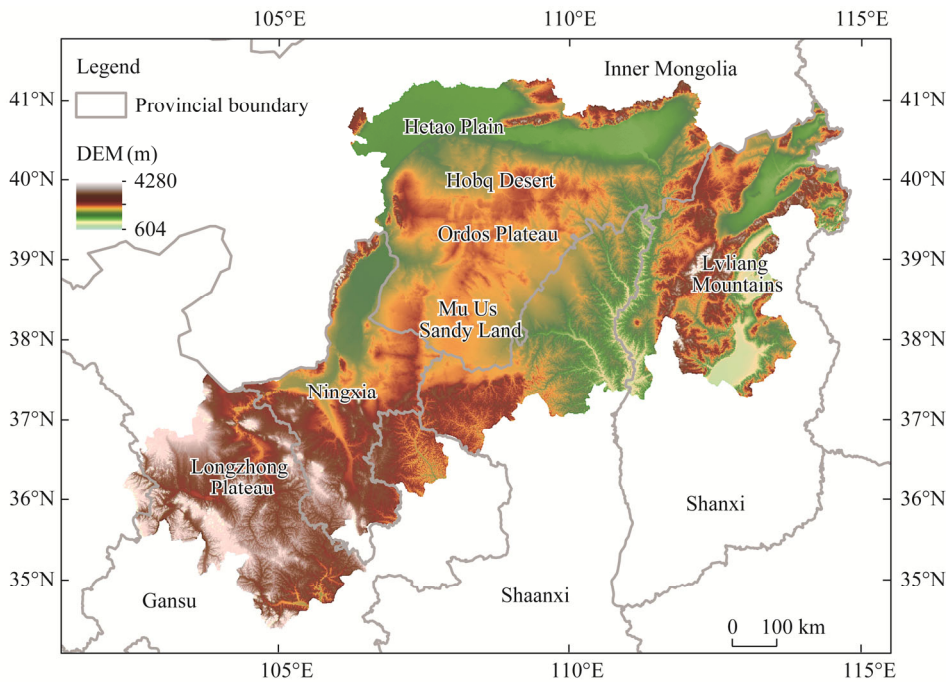

Fig. 1 Location and digital elevation model (DEM) of the wind-water erosion area of Chinese Loess Plateau. Note that the figure is based on the standard map (GS(2022)4309) of the Map Service System (https://bzdt.ch.mnr.gov.cn/), and the boundary has not been modified.

2.2 Data sources

Fundamental datasets included meteorological and remote sensing data (Table 1). Meteorological data comprised hourly wind speed and monthly precipitation recorded at meteorological stations. Hourly wind speed data were obtained from the National Climatic Data Center (NCDC;

https://www.ncdc.noaa.gov/cdo-web/). Time series of 50 sites during 2000–2020 and cumulative time of wind speed greater than (equal to) the critical erosion wind speed (5.0 m/s) were obtained statistically. Precipitation data were acquired from the China Meteorological Science Data Sharing Service Network (http://cdc.cma.gov.cn/home.do), and monthly data recorded during 2000–2020 at 257 stations within and surrounding the study area were selected. Meteorological data were interpolated into raster data with spatial resolution of 1 km×1 km using ANUSPLINE software.

Remote sensing data included land use, soil type, normalized difference vegetation index (NDVI), digital elevation model (DEM), and boundaries. Land use data during 2000–2020 were derived from the China Land Cover Dataset of Wuhan University (http://doi.org/10.5281/zenodo.4417810), with a spatial resolution of 30 m×30 m. Soil type with the scale of 1:1,000,000 was derived from the Resources and Environmental Science and Data Center, Chinese Academy of Sciences (CAS; http://www.resdc.cn/). NDVI were downloaded from the United States Geological Survey (http://glovis.usgs.gov/). DEM, which was based on shuttle radar topography mission data with a spatial resolution of 30 m×30 m, was derived from the Geospatial Data Cloud (https://www.gscloud.cn/). All the raster data were resampled into a spatial resolution of 1 km×1 km. Additionally, the boundary of wind erosion areas in northern China and the Loess Plateau were derived from the Water Conservancy Census of China and Resources and Environmental Science and Data Center, CAS, respectively.

Table 1 Data information and sources

Data type	Date	Resolution	Processing	Data source
Meteorological data	Hourly wind speed	1 km×1 km	Using ANUSPLINE, meteorological data were interpolated to raster data	National Climate Data Center
	Monthly precipitation	1 km×1 km		China Meteorological Science Data Sharing Service Network
Remote sensing data	LULC	30 m×30 m	LULC, soil type, NDVI, and DEM data were uniformly processed into raster data with a spatial resolution of 1 km×1 km	Wuhan University's Annual China Land Cover Dataset (CLCD)
	Soil type	1:1,000,000		Resources and Environmental Science and Data Center, Chinese Academy of Sciences
	NDVI	MODIS 1 km/16d		United States Geological Survey
	DEM	30 m×30 m		Geospatial Data Cloud
	Boundary of wind erosion area in northern China	Vector		Water Conservancy Census of China
	Boundary of Loess Plateau	Vector		Resources and Environmental Science and Data Center, Chinese Academy of Sciences

Note: LULC, land use and land cover; NDVI, normalized difference vegetation index; DEM, digital elevation model; MODIS, moderate resolution imaging spectroradiometer.

2.3 Methods

2.3.1 Soil protection assessment model

Soil protection is the sum of soil erosion reduction amount by wind and water and calculated by the following equation:

$$G_{SP} = G_{wind} + G_{water}, \tag{1}$$

where G_{SP}, G_{wind}, and G_{water} are the soil protection amount, wind erosion reduction amount, and water erosion reduction amount (t/(hm^2·a)), respectively.

Wind erosion reduction amount is the difference between actual wind erosion amount under conditions of plant protection and potential wind erosion amount in the absence of plants (Cui et al., 2023) and calculated as follows:

$$G_{wind} = Q_{pwind} - Q_{awind}, \tag{2}$$

where Q_{pwind} and Q_{awind} are the potential and actual wind erosion amount (t/(hm^2·a)), respectively.

Q_{pwind} and Q_{awind} are estimated by National Wind Erosion Survey Model of China (Zhao et al., 2023). It is an empirical model used for predicting wind erosion in northern China based on measured data. The model considers the impact of land use, and it includes three sub-models, i.e., the cultivated land model, grassland (shrub land) model, and sandy land model. The sub-models are expressed as follows:

$$Q_{wc} = 0.018\sum_{i=1} T_i \exp\left\{a_1 + \frac{b_1}{z_0} + c_1\left[\left(Au_i\right)^{0.5}\right]\right\}, \tag{3}$$

$$Q_{wgs} = 0.018\sum_{i=1} T_i \exp\left[a_2 + b_2 V^2 + c_2 / (Au_i)\right], \tag{4}$$

$$Q_{ws} = 0.018\sum_{i=1} T_i \exp\left[a_3 + b_3 V + c_3 \frac{\ln(Au_i)}{Au_i})\right], \tag{5}$$

where Q_{wc}, Q_{wgs}, and Q_{ws} are the wind erosion amount of cultivated land, grassland (shrub land), and sandy land (t/(hm^2·a)), respectively; T_i is the i^{th} cumulative time (min); z_0 is the surface aerodynamic roughness (cm); A is the wind speed modification factor associated with the surface (m/s); u_i is the i^{th} wind speed (m/s); V is the vegetation coverage (%); and the values of a_1, b_1, and c_1 are 9.208, 0.018, and 1.955, respectively; a_2, b_2, and c_2 are 2.487, –0.001, and –54.947, respectively; a_3, b_3, and c_3 are 6.169, –0.074, and –27.961, respectively (Li et al., 2013).

Sediment retention module in the InVEST model was used to calculate sediment by water erosion (G_{water}) (Li et al., 2023):

$$G_{water} = Q_{pwater} - Q_{awater} + S_{DR}, \tag{6}$$

where Q_{pwater} is the potential water erosion amount in the absence of plants, management, and water and soil conservation measures (t/(hm^2·a)); Q_{awater} is the actual water erosion amount (t/(hm^2·a)); and S_{DR} is the sediment retention (t/(hm^2·a)). Q_{pwater} and Q_{awater} are calculated by the revised universal soil loss equation, which are suitable for the hydraulic erosion simulation on the Loess Plateau (Ed-daoudy et al., 2023; Li et al., 2024). The above indices are calculated by the following equations:

$$Q_{pwater} = R \times K \times LS, \tag{7}$$

$$Q_{awater} = R \times K \times LS \times C \times P, \tag{8}$$

$$S_{DR} = SE \times \sum Q_{awater} \prod (1 - SE_u), \tag{9}$$

where R is the precipitation erosion factor (MJ·mm/(hm^2·h·a)) derived from the Wischmeier's formula using monthly and annual precipitation (Wischmeier et al., 1971); K is the soil erodibility factor (t·h/(MJ·mm)) computed using the formula of Williams et al. (1984); LS is the slope factor; C is the vegetation coverage and management factor; P is the factor of soil and water conservation measures (Mu et al., 2022); and SE and SE_u are the efficiency of sediment retention rate in this raster and upslope raster u, respectively.

Soil retention rate (F; %) is defined as the ratio of soil protection amount (G; t) to potential soil erosion amount (Q_p; t). It is an important indicator for evaluating soil protection, which eradicates the impact of inter-annual precipitation fluctuation on the simulation result (Li and Xu, 2019):

$$F = G / Q_p \times 100\%. \tag{10}$$

According to above principle, we separately calculated soil protection retention rate (F_1), reduced wind erosion retention rate (F_2), and reduced water erosion retention rate (F_3).

2.3.2 Analytical method of trade-off and synergy

Relationship between wind and water erosion reduction is quantitatively evaluated by pixel-by-pixel partial correlation spatiotemporal statistical mapping (Huang and Wu, 2023). The reductions of wind erosion and water erosion in the simulation are affected by precipitation and vegetation coverage. In order to better evaluate the spatial relationship between them, we calculated the partial correlation coefficient under the condition of constant precipitation and vegetation

coverage.

2.3.3 Bivariate spatial autocorrelation analysis

Bivariate spatial autocorrelation analysis was used to analyze the spatial correlation between wind speed, slope, precipitation, vegetation coverage, and soil protection. Moran's *I* index and local indicators of spatial association (LISA) cluster map were obtained by computer mapping. The value of Moran's *I* value ranges from –1 to 1. Moran's $I>0$ represents a positive correlation between variables; Moran's $I<0$ means that the variables are negatively correlated; and Moran's $I=0$ means that the variables do not pass the significance test. Spatial random distribution is displayed among these variables. According to the local spatial correlation among variables, we divided LISA cluster plots into high-high (H-H), low-low (L-L), high-low (H-L), low-high (L-H), and not significant (NS). H-H and L-L types are positively correlated, and H-L and L-H are negatively correlated (Wu et al., 2023).

2.3.4 Cellular automata (CA)-Markov model

CA-Markov model is often used to simulate and predict the change of land use type (Malathy and Bhaskar, 2023). Based on the land use in 2015, we adopted CA-Markov model to predict the land use pattern in 2030 under three different scenarios: (1) business as usual (BAU) scenario: land use pattern in 2030 is obtained under natural evolution process of Markov chain without considering natural conditions and human factors changes; (2) economic growth (EG) scenario: the conversion of construction land and transportation land is forbidden, part cultivated land, forest land, and grassland are set as convertible land, and the possibility of converting unused land into residential land increases. Elevation and slope are selected as suitable factors, and the values are less than 1300 m and 1°, respectively; and (3) ecological conservation (EC) scenario: ecological land (water body, forest land, and grassland) is set as restricted land type. Elevation and slope are selected as suitable factors again. Cultivated land and construction land with slope >7° and elevation >2000 m are converted into forest land and grassland, respectively.

3 Results

3.1 Spatial and temporal characteristics of soil protection

Total soil erosion, wind erosion, and water erosion in the wind-water erosion area of the Loess Plateau during 2000–2020 were 14.21×10^8, 8.17×10^8, and 6.04×10^8 t, respectively (Fig. 2). The average soil erosion amount was 38.50 t/(hm^2·a), and the average wind erosion and water erosion amount were 22.14 and 16.36 t/(hm^2·a), respectively. During the past 21 a, soil protection effect of the wind-water erosion area of the Chinese Loess Plateau was remarkable, and the total amount reached 15.47×10^8 t. During 2000–2020, the amount of soil protection increased at a rate of 0.69 t/(hm^2·a) (Fig. 2a), and soil protection retention also increased at a rate of 0.57%/a (Fig. 2d), indicating that soil erosion was effectively controlled and the effect of soil protection was gradually enhanced. Total amount of wind erosion reduction was 5.68×10^8 t, which decreased at a rate of –0.10 t/(hm^2·a) (Fig. 2b), but wind erosion reduction increased at a rate of 0.49%/a, which was benefit by the increase in vegetation (Fig. 2e). In addition, total amount of water erosion reduction was 9.79×10^8 t, increasing at a rate of 0.80 t/(hm^2·a) (Fig. 2c), and water erosion reduction also continued to increase at a rate of 0.29%/a (Fig. 2f). Soil conservation capacity gradually improved, which protected the local land resources and ecological environment.

Wind-water erosion area of the Loess Plateau is facing great challenges in soil protection and ecological restoration. About 63.70% of the total soil protection was low (Fig. 3). The medium and high levels of soil protection was concentrated in the Mu Us Sandy Land, accounting for 36.30% (Fig. 3a), and the areas with soil retention rate of more than 40.00% were mostly located in the northern Mu Us Sandy Land and northern Shanxi Province (Fig. 3d), where achieved good effects with the Grain for Green and grassland ecological measures. Wind erosion reduction in the northern Loess Plateau was generally low, and the high value area was concentrated in the Mu Us Sandy Land and eastern Hobq Desert (Fig. 3b). Only 20.30% of the areas with the retention rate

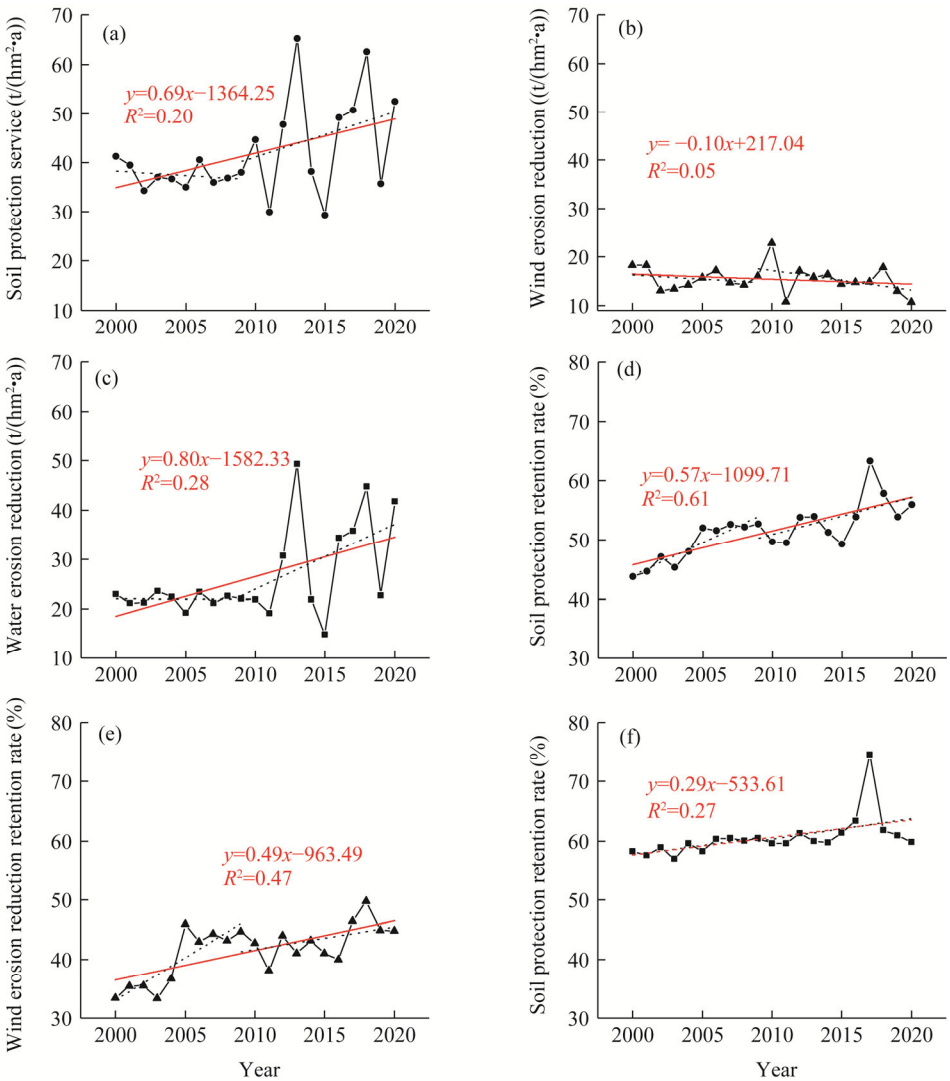

Fig. 2 Inter-annual variations in soil protection service (a), wind erosion reduction (b), water erosion reduction (c), soil protection retention rate (d), wind erosion reduction retention rate (e), and soil protection retention rate (f). Red lines and functions represent the overall trend lines and trend functions for each parameter during 2000–2020, respectively; and black dashed lines represent the overall trend lines for each parameter during 2000–2009 and 2010–2020.

of wind erosion reduction was more than 40.00%, concentrated in the Mu Us Sandy Land and central of Ordos Plateau (Fig. 3e). Water erosion reduction was also low, and the area with high value was located in the northern Shanxi Province and southern Longzhong Plateau (Fig. 3c). The areas that the retention rate of water erosion reduction exceeded 40.00% accounted for 72.30%, concentrated in northern Ordos Plateau and central and western Longzhong Plateau (Fig. 3f). Soil erosion in the study area had cross-regional characteristics. Overall, prevention and control measures for soil protection were effective and could be further continued.

During the past 21 a, inter-annual variation of soil protection in the wind-water erosion area of the Loess Plateau showed significant spatial differences (Fig. 4). About 51.20% of the area showed an increasing trend, concentrated in the middle Mu Us Sandy Land; 35.50% of the changes were not obvious, mainly located in the Hetao Plain and northern Ningxia Hui Autonomous Region (Fig. 4a). Soil conservation rate of 71.00% showed an increasing trend, of which 56.10% showed a slight increase. About 24.10% showed a decreasing trend, mainly in the

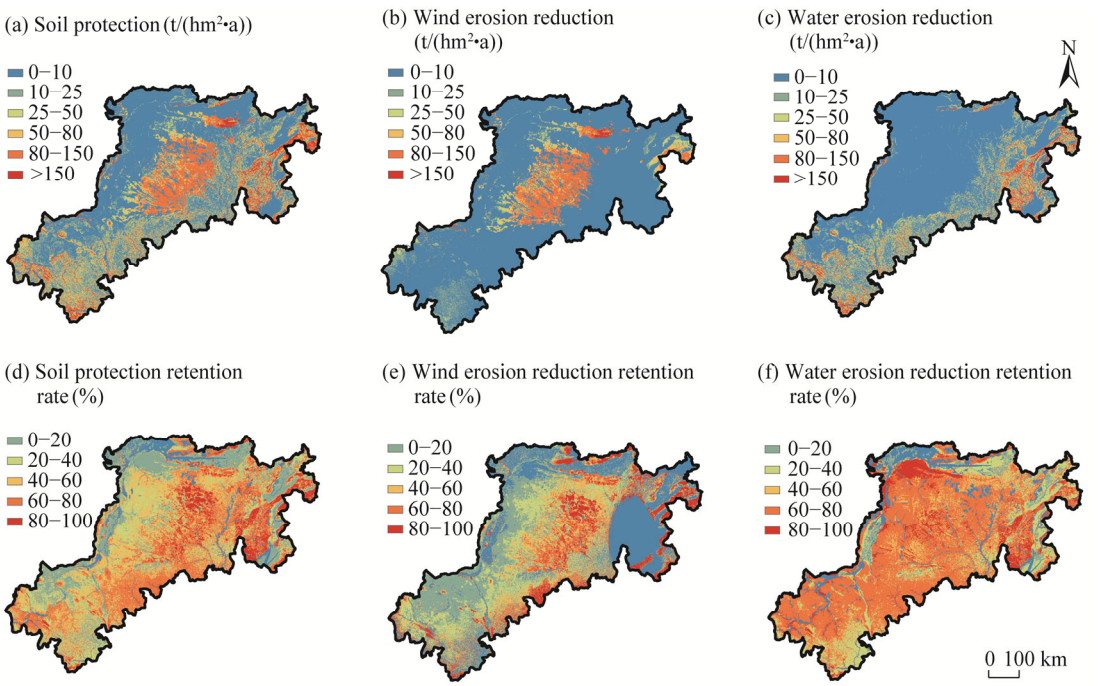

Fig. 3 Spatial patterns of soil protection (a), wind erosion reduction (b), water erosion reduction (c), soil protection retention rate (d), wind erosion reduction retention rate (e), and water erosion reduction retention rate (f) in the wind-water erosion area of the Loess Plateau during 2000–2020

Hetao Plain. Change of 4.90% was not significant and was mainly distributed in the Hobq Desert (Fig. 4d). Anthropogenic disturbance had significant effects on soil erosion and protection, including positive effects in ecological areas (e.g., Mu Us Sandy Land) and negative effects in agricultural areas (e.g., Hetao Plain). However, the Hobq Desert itself has poor soil and is affected by natural environment such as wind speed, which still needs to continue to strengthen ecological protection and restoration work to prevent further expansion of desertification. The area with a decreasing trend of wind erosion accounted for 37.00%, and the area with a significant decrease accounted for 15.90%, which distributed in the middle Hobq Desert and northern and southern Mu Us Sandy Land. The area increased by 7.20%, mainly in southern Gansu Province. About 55.80% of the changes were not obvious, mainly in Ningxia Hui Autonomous Region and Hetao Plain (Fig. 4b). Retention rate increased by 15.40%, mainly in the Ordos Plateau. Retention rate decreased by 11.10% in northern Ningxia Hui Autonomous Region. The change of 73.50% was not obvious, mainly in central Ordos Plateau (Fig. 4e). Decrease of water erosion was increasing significantly, accounting for 40.70%, mainly in Gansu Province, southern Longzhong Plateau, and northern Shanxi Province (Fig. 4c). Decreasing trend was only 0.20%; and there was no significant change in central Hetao Plain (59.10%). About 85.90% of the area showed an increasing trend in retention rate of water loss, concentrated in the Ordos Plateau, 10.97% of the area showed a decreasing trend, mainly distributed in the Hetao Plain, and 3.13% changes were not significant, mainly in the Hobq Desert (Fig. 4f). On the whole, there were regional differences in the trend of water erosion reduction and retention rate. Gansu Province, southern Longzhong Plateau, and northern Shanxi Province had achieved remarkable effects in soil and water conservation, while the Hetao Plain and other agricultural areas should be strengthened. Ecologically fragile region, such as the Hobq Desert, needs continuous attention to ensure ecological stability and sustainable development.

3.2 Trade-off and synergy

Relationship between wind erosion reduction and water erosion reduction during 2000–2020 was

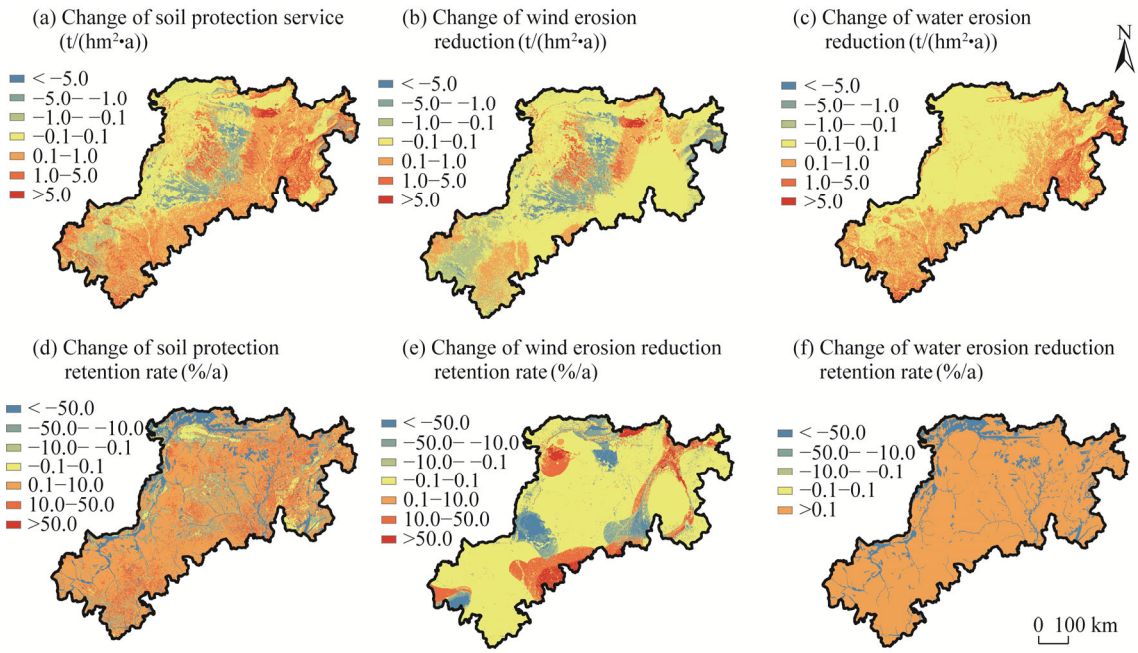

Fig. 4 Changes of soil protection service (a), wind erosion reduction (b), water erosion reduction (c), soil protection retention rate (d), wind erosion reduction retention rate (e), and water erosion reduction retention rate (f) in the wind-water erosion area of the Loess Plateau during 2000−2020

dominated by synergy, with a synergy relationship and synergy area of 0.044 and 41.61%, respectively. Area of highly significant synergy accounted for 37.68% of the total, concentrated in the windy and sandy area in northern Shaanxi Province and western Mu Us Sandy Land. Trade-off area accounted for 26.05% of the total, with area of insignificant trade-off accounting for 24.66%, distributed in southern Ordos Plateau, Longzhong Plateau, central and eastern Ningxia Hui Autonomous Region, and central Hobq Desert. The areas with a significant and highly significant trade-off relationship accounted for only 1.39% of the total, concentrated in southern Mu Us Sandy Land (Fig. 5). Increase in vegetation coverage is beneficial for inhibiting soil erosion, but intense plant transpiration will consume large quantity of water, which is not abundant in central and northern Loess Plateau. Thus, appropriate vegetation coverage and low water consuming plants should be considered during vegetation restoration.

Land use type, elevation, and slope can also influence soil erosion and soil protection in the Loess Plateau. The trade-off and synergy interactions between wind erosion reduction and water erosion reduction under various land use patterns are shown in Figure 6. For most land use types (except water body), synergy relationships were more dominant than trade-off relationships, and highly significant synergy relationships and nonsignificant trade-off relationships were dominant. In terms of synergy relationship, the proportions of grassland, unused land, and forest land were 51.03%, 33.55%, and 33.94%, respectively; and extremely significant synergy relationships accounted for 46.25%, 30.60%, and 30.93%, respectively. The proportions of trade-off relationships for grassland, unused land, and cultivated land were 31.56%, 22.49%, and 16.56%, respectively, and the nonsignificant trade-off relationships accounted for 29.90%, 20.73%, and 15.68%, respectively (Fig. 6a). Trade-off and synergy interactions between wind erosion reduction and water erosion reduction at various elevations are shown in Figure 6b. Altitudes of 600–1200 and >2400 m exhibited mainly trade-off relationships, whereas altitudes of 1200–2400 m exhibited mainly synergy relationships. Trade-off and synergy relationships between wind erosion reduction and water erosion reduction under different slopes are shown in Figure 6c. The area with 16°–24° slope was dominated by trade-off relationships, accounting for more than

30.00% of the total, whereas the remaining areas were dominated by synergy relationships. With increase in slope, the synergies between soil protection showed a downward trend, and vice versa. Rational vegetation restoration on steep slopes could enhance wind erosion reduction and improve soil protection capability.

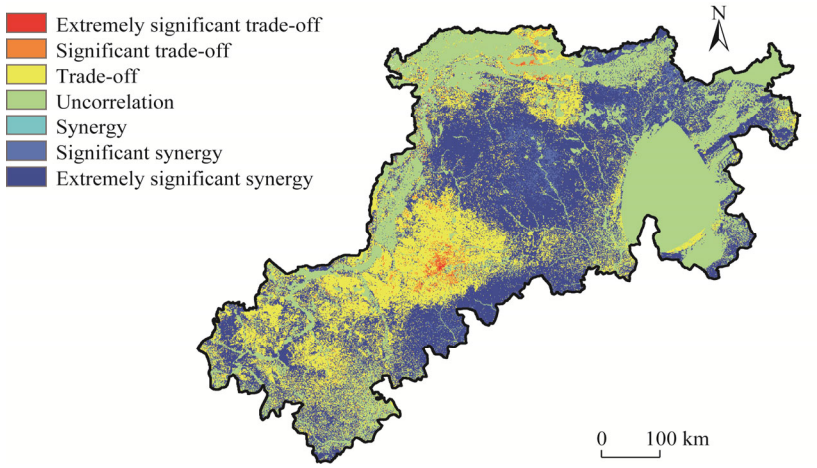

Fig. 5 Spatial relationship between wind erosion reduction and water erosion reduction

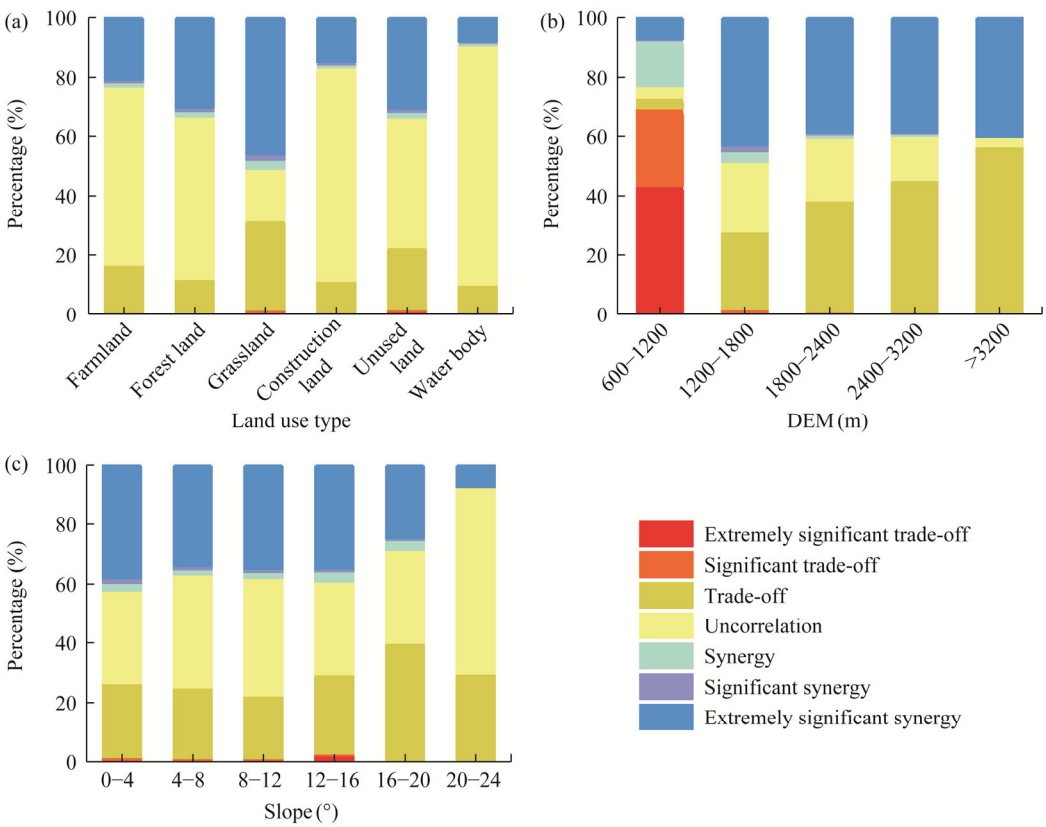

Fig. 6 Trade-off and synergy between wind erosion reduction and water erosion reduction under different land use types (a), digital elevation model (DEM; b), and slopes (c)

3.3 Influencing factors

3.3.1 Natural factor

When wind speed threshold of 5.0 m/s is exceeded, wind speed has substantial impact on soil

wind erosion. When wind speed cumulative time decreases, sand fixation capacity decreases, the wind erosion reduction retention rate increases, and wind erosion reduction is enhanced. Wind speed cumulative time (≥5.0 m/s) was significantly and positively correlated with wind erosion reduction, and the Moran's *I* index was 0.055 (P<0.001). Positive correlation accounted for 49.99% of the total, dominated by L-L type, which corresponded to the spatial pattern of wind speed. Sand fixation capacity decreased in the area with low wind speed cumulative time (≥5.0 m/s). H-H type accounted for only 2.64%, distributed mainly in the middle Mu Us Sandy Land and northern Shanxi Province. The area with negative correlation accounted for 16.42%, mainly L-H type (10.85%), distributed in the Mu Us Sandy Land and eastern Hobq Desert. H-L type was distributed mainly in central Ningxia Hui Autonomous Region (Fig. 7a).

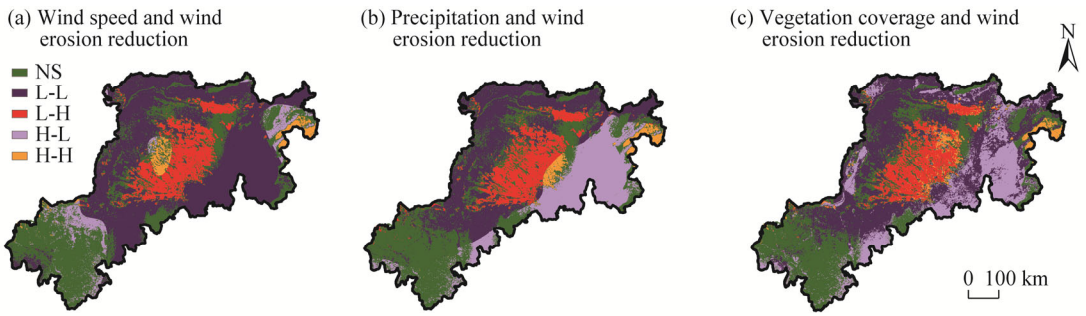

Fig. 7 Local indicators of spatial association (LISA) plots of wind speed and wind erosion reduction (a), precipitation and wind erosion reduction (b), and vegetation coverage and wind erosion reduction (c). NS, not significant; L-L, low-low; L-H, low-high; H-L, high-low; H-H, high-high. The abbreviations are the same in Figure 8.

There was positive correlation between precipitation and wind erosion reduction, and the Moran's *I* index was 0.059 (P<0.001; Fig. 7b). There was negative correlation between vegetation coverage and wind erosion reduction, and the Moran's *I* index was –0.145 (P<0.001). The spatial relationship between precipitation and wind erosion reduction was dominated by L-L and L-H types; the former was distributed mainly in northern Shaanxi and northwestern Gansu provinces, and southwestern Inner Mongolia Autonomous Region, and the latter was distributed in the Mu Us Sandy Land and Hobq Desert (Fig. 7b). The area with positive correlation between vegetation coverage and wind erosion reduction accounted for 38.74% of the total, mainly L-L type (35.94%), distributed in western Ordos Plateau, Hetao Plain, and central Ningxia Hui Autonomous Region. The area with negative correlation was 29.04% of the total, mainly L-H type (10.38%), concentrated in eastern Mu Us Sandy Land and Hobq Desert (Fig. 7c). The increase in precipitation and vegetation coverage effectively reduced wind speed, resulting in gradual decrease in the number of hours with wind speed initiating sand movement, wind erosion intensity, and sand fixation capacity.

Negative correlation was found between precipitation and water erosion reduction, with the Moran's *I* index of –0.044 (P<0.001), and positive correlation was found of vegetation coverage and slope with water erosion reduction with the Moran's *I* index of 0.045 (P<0.001) and 0.015 (P<0.001), respectively. Both slope and vegetation coverage had great influence on water erosion reduction. Spatial relationships of precipitation, vegetation coverage, and water erosion reduction were mainly L-L and H-L types. L-L type was distributed mainly in southern Inner Mongolia Autonomous Region, northern Ningxia Autonomous Region, and northwestern Gansu province. H-L type was concentrated in northern Lvliang Mountains (Fig. 8a and b). Spatial relationship between slope and water erosion reduction was dominated by L-L and H-H types. L-L type was distributed mainly in northern Ordos Plateau and northern Ningxia Hui Autonomous Region, whereas H-H type was scattered in northern Shanxi Province (Fig. 8c).

3.3.2 Land use/land cover

Main land use types in the wind-water erosion area of the Loess Plateau were grassland and

cultivated land. Overall, grassland accounted for 63.70% of the total area, followed by cultivated land (24.90%), and then construction land, forest land, water body, and unused land. From the perspective of spatial pattern, grassland was mainly concentrated in central and western parts of the study area, whereas cultivated land was scattered in the plains. All land use types showed notable change during 2000–2020 (Table 2), with the areas of grassland, forest land, and water body increasing by 3.68%, 0.67%, and 0.11%, respectively. The areas of unused land, construction land, and cultivated land decreased by 2.96%, 9.49%, and 2.7%, respectively. During the past 21 a, 36,437 km^2 of forest land were converted into grassland, and 29,296 km^2 of grassland were converted into cultivated land (Table 2). Grassland reclamation continued despite the grassland area increased. The increases in forest land and grassland had enhanced regional vegetation coverage, which was conducive to reducing the wind erosion and water erosion.

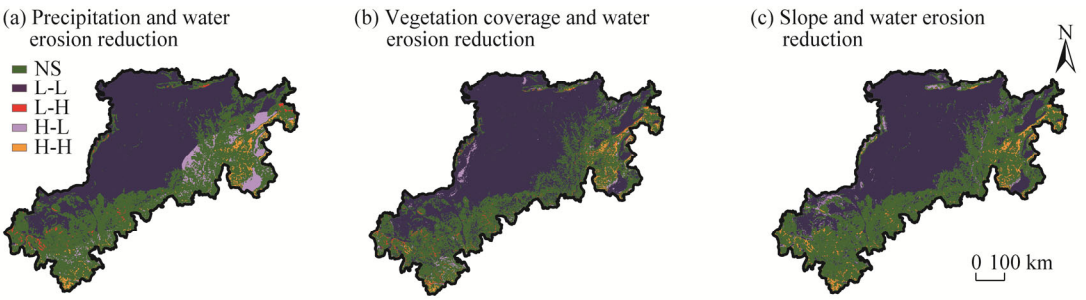

Fig. 8 Localized LISA plots of precipitation and water erosion reduction (a), vegetation coverage and water erosion reduction (b) , and slope and water erosion reduction (c)

Table 2 Land use area transfer matrix from 2000 to 2020

Land use type	Farmland	Forest land	Grassland	Water body	Construction land	Unused land	Decreasing area
				(km^2)			
Farmland	56,228	1030	36,437	619	208	0	38,294
Forest land	313	7025	3743	6	8	0	4070
Grassland	29,296	5420	171,721	482	5185	1953	42,336
Water body	445	15	279	661	35	128	902
Construction land	1152	0	14,416	122	11,489	343	16,033
Unused land	1262	0	1814	70	39	776	3185
Increasing area	32,468	6465	56,689	1299	5475	2424	-

Note: "-" means no value.

Changes in wind erosion reduction and water erosion reduction in 2030 under BAU, EC, and EG scenarios are shown in Figure 9. Sand fixation capacity per unit area was as follows: EG scenario (15.52 t/(hm^2·a))>EC scenario (15.42 t/(hm^2·a))>BAU scenario (15.33 t/(hm^2·a)). Compared with 2020, sand fixation capacity per unit area is expected to increase in all three scenarios. Sand fixation capacity per unit area was projected to increase by 44.37% under EG scenario, attributable to the rapid economic growth, substantial expansion of construction land, and large amount of ecological land occupation. Water erosion reduction per unit area was as follows: EC scenario (30.02 t/ (hm^2·a))>EG scenario (25.94 t/(hm^2·a))>BAU scenario (21.44 t/(hm^2·a)). Water erosion reduction per unit area was expected to decrease in all three scenarios compared with the situation in 2020. If ecological protection measures were taken to limit the diversion of forest land, grassland, and water body in EC scenario, the decrease of water erosion reduction per unit area would be only 11.74 t/(hm^2·a) owing to the reduction in farmland. Therefore, ecological protection measures should be taken on the basis of cultivated land protection to prevent further expansion of construction land and to enhance soil protection.

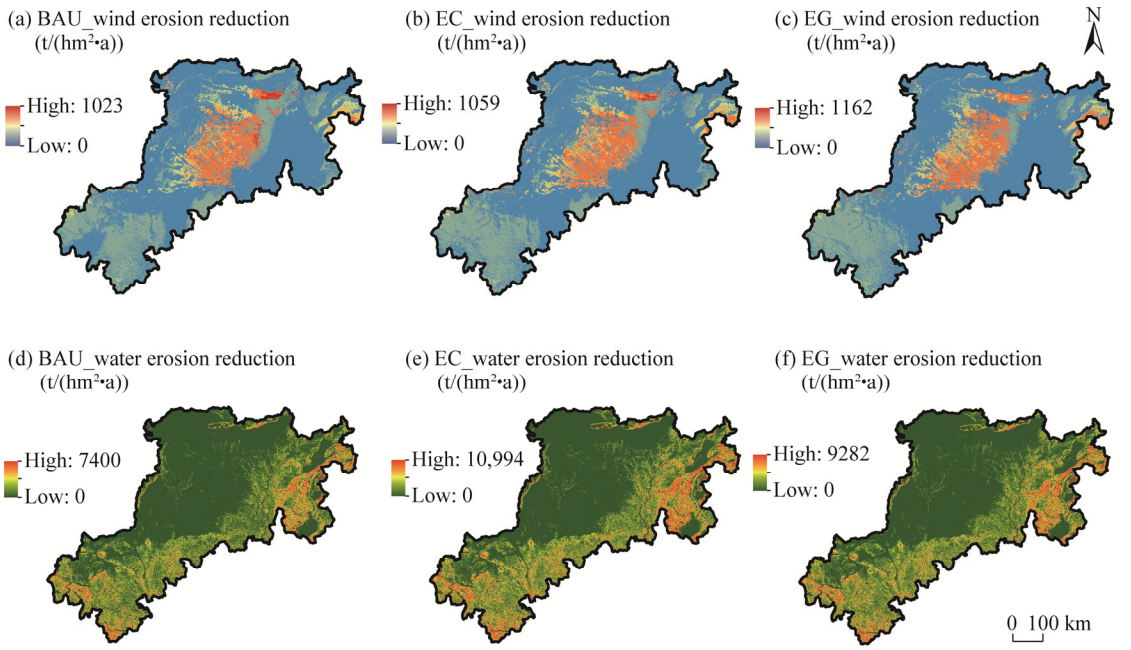

Fig. 9 Changes in wind erosion reduction and water erosion reduction under three scenarios (business as usual (BAU; a and d), ecological conservation (EC; b and e), and economic growth (EG; c and f))

4 Discussion

4.1 Evaluation indicators of soil protection

Water erosion reduction (assessing soil and water conservation) and wind erosion reduction (assessing windbreak and sand fixation) can directly reflect the ability of vegetation to reduce soil erosion under current climate conditions (Wang et al., 2023c). However, they are susceptible to climatic factors, such as wind speed and precipitation. Because the protective effect of an ecosystem might be underestimated or overestimated, these two indicators are hard to truly represent the ecosystem effect on soil protection (Huang et al., 2022; Yang et al., 2023). During 2000–2020, vegetation coverage in the study area showed an upward trend, and annual wind erosion decreased by 7.52 t/(hm^2•a) (Fig. S1). However, wind erosion reduction has shown a decreasing trend owing to the notable decrease in wind speed. The result means that the indicator has certain limitation for evaluating the soil erosion reduction of vegetation.

Soil retention rate can eliminate the effects of climate change (i.e., precipitation and wind speed) to a certain extent, and thus can objectively reflect the soil protection of ecosystems (Li and Xu, 2019; Gong et al., 2020). In this study, wind erosion retention rate in 2000 (33.39%) was obviously lower than that in 2020 (44.77%), which is consistent with the increasing trend of vegetation coverage. Wind erosion retention rate can objectively reflect the potential of vegetation to prevent wind and fix sand. However, soil retention rate was difficult to evaluate soil erosion reduction amount in some extreme climate conditions. Therefore, these two indicators (the amount and retention rate of soil erosion reduction) should be combined in subsequent studies to comprehensively evaluate the ability of vegetation/climate to reduce soil erosion.

4.2 Future changes of soil erosion

Relative to water erosion, wind erosion in northern Loess Plateau was more serious. Average wind erosion amount (22.14 t/(hm^2•a)) was greater than water erosion amount (16.36 t/(hm^2•a)) during 2000–2020 (Fig. S1). As a direct driving force for regional soil-wind erosion, wind speed (especially the frequency of strong winds) in northern Loess Plateau showed a notable decreasing

trend, especially in winter and spring (Xiao and An, 2023). As a result, the inter-annual wind erosion amount revealed a decline trend, with a rate of –0.64 t/(hm^2·a). However, the inter-annual water erosion showed an increasing trend, with a rate of 0.31 t/(hm^2·a) (Fig. S1). Driving force analysis showed that precipitation and vegetation are the most important factors on water erosion. Precipitation is the direct external force for soil-water erosion, especially extreme rainfall has the greatest effect on soil dispersion and destruction (Zhang et al., 2023b; Li et al., 2024). Annual precipitation showed a significantly increasing trend in the wind-water erosion area of the Loess Plateau, increasing from 415.80 mm/a during 2000–2009 to 463.44 mm/a during 2010−2020. The rainfall erosivity and water erosion increased with increasing precipitation. Most of water erosion amounts in the Loess Plateau were caused by a few extreme rainfall events (Fu, 1989). Soil erosion caused by a single extreme rainfall event was equivalent to 40.00%–90.00% of the annual erosion (Tang et al., 1992). Recently, the occurrence of extreme rainfall events increased significantly (Li et al., 2022; Zhang et al., 2023b; Li et al., 2024), which led to substantial increase in soil-water erosion (Zhang et al., 2023b). With climate changes (i.e., reduced wind speed and increased precipitation), wind erosion was weakened in 81.44% of the study area, while water erosion was strengthened in 52.83% of the study area. Water erosion exceeded wind erosion in the late 2010s and became the main type of soil erosion. The predictions of global climate models in CMIP6 (Coupled Model Intercomparison Project Phase 6) show that the near-surface wind speed in northern China will decrease further in the future (Eyring et al., 2016; Wu et al., 2020), which will be conducive to the weakening of soil-wind erosion. Predictions of global climate models in CMIP5 (Coupled Model Intercomparison Project Phase 5) show that annual precipitation and intensity and frequency of extreme precipitation events will increase significantly (Wang et al., 2023b; Li et al., 2024), which will be conducive to soil-water erosion. It can be inferred that soil-water erosion will become the main soil erosion form in the wind-water erosion area of the Loess Plateau, and its contribution may be enhanced in the future. Although vegetation restoration has played an important role in preventing soil erosion, the impact of climate changes may be greater than that of vegetation. Therefore, it is necessary to pay more attention to the prevention and control of soil-water erosion in the study area (Fu et al., 2017).

4.3 Future soil conservation proposals

Under the combined influence of socioeconomic and biophysical factors, the trade-off and synergy during soil protection process revealed spatial heterogeneity. Spatial relationships between wind erosion reduction and water erosion reduction were weak in the Hetao Plain, Yinchuan Basin, and central Shanxi Province where were main agricultural planting areas in the wind-water erosion area of the Loess Plateau. In these areas, the terrain is low and flat, the water resources are abundant owing to adjacent rivers, and the vegetation is mainly composed of crops. The soil erosion modulus is less than 25.00 t/(hm^2·a) (Fig. S2). Underlying surface is bare in spring, and wind erosion is prone to occur. It is suggested that high-standard farmland shelterbelts construction should be strengthened, conservation-focused farming should be promoted, and regional advantages should be exploited in developing irrigation agriculture and other suitably advantageous industries (Zhao et al., 2020). Shelterbelt structure parameters are the key factors affecting the efficiencies of windbreak and sand fixation (Zhu et al., 2003; Wu et al., 2013). Sai (2022) reported that the protection efficiency of trees and shrubs mixed planting is better than that of pure trees planting. Thus, the trees and shrubs mixed planting should be given priority consideration during future farmland shelterbelt construction. The synergistic relationship was extremely significant between wind erosion reduction and water erosion reduction in southeastern Inner Mongolia and southeastern Ningxia Hui autonomous regions, and northern Shaanxi, western Shanxi, and northwestern Gansu provinces. In these areas, hills and gullies are widely distributed, the slope is large, and annual precipitation is more than 300 mm. Soil erosion modulus in some areas is larger than 25.00 t/(hm^2·a) (Fig S2). Meanwhile, vegetation in these areas was quickly recovered in the wind-water erosion area of the Loess Plateau in past decades (Yang et al., 2019). It is recommended to take vegetation restoration as the focus of future strategies, to strengthen vegetation restoration enclosures, and to ban and postpone grazing (Bai et

al., 2024; Guo et al., 2024). Check-dams and terraces are effective engineering measures to prevent gully erosion, and mainly used in small channel basin with an area of 100–200 km^2 (Wen and Zhen, 2020). Engineering measures can also be implemented in above areas. Moreover, the selection and setting of vegetation must meet the regional water resources carrying capacity (Jia et al., 2017; Wen and Zhen, 2020). Wind erosion reduction and water erosion reduction showed trade-off relationships in northwestern Shaanxi and western Gansu provinces, and central Ningxia Hui and southwestern Inner Mongolia autonomous regions where are fragmented areas with high terrain, large elevation variation, and concentrated precipitation. It is suggested that comprehensive management of small watersheds should be undertaken in the future, with treatments to protect gully head near the gully edge line, construction of check dams in dry gully, adoption of terracing on slopes, and restoration vegetation (Liu et al., 2020; Guan et al., 2023).

5 Conclusions

In this study, the spatiotemporal patterns, spatial relationships, and driving factors of soil protection were comprehensively analyzed in the wind-water erosion area of the Chinese Loess Plateau during 2000–2020. The total amount of soil protection was 15.47×10^8 t, in which the reduction of wind erosion and water erosion were 5.68×10^8 and 9.79×10^8 t, respectively, and the soil protection retention rate reached 51.50%. Inter-annual variation of wind erosion reduction showed a decreasing trend, while soil protection amount, water erosion reduction, and soil protection retention rate showed increasing trends. Spatial classification of total soil protection amounts was mainly L-L type, and concentrated in the Mu Us Sandy Land, and southwestern Gansu and northern Shanxi provinces. Synergistic relationship between wind erosion reduction and water erosion reduction was dominant, and trade-off relationship was mainly distributed in southern and northern study area. Wind speed was the main climate factor affecting wind erosion reduction, while precipitation, vegetation, and slope were important factors affecting water erosion reduction. Land use change and implementation of ecological engineering measures were also important reasons for reducing wind erosion and water erosion. This study deeply revealed the dynamic evolution and driving mechanism of soil protection in the wind-water erosion area of the Loess Plateau. Meanwhile, an effective assessment framework and methodology was proposed to provide valuable reference for other areas worldwide facing wind-water erosion.

Conflict of interest

The authors declare that they have no known competing financial interests or personal relationships that could have appeared to influence the work reported in this paper.

Acknowledgements

This research was funded by the National Key Research and Development Program of China (2023YFF1305304), the National Natural Science Foundation of China (41801007), the Second Tibetan Plateau Scientific Expedition and Research Program (2019QZKK0201), the Science Technology Project of Hebei Academy of Sciences (2024PF11), the Basic Research Program of Shanxi Province (202203021211258, 202103021223248), and the Science and Technology Strategy Project of Shanxi Province (202304031401073).

Author contributions

Methodology: LI Qing, LI Dan; Data curation: LI Qing, WANG Sheng, WANG Rende, FU Gang; Investigation: LI Qing, WANG Rende, FU Gang, YUAN Yixiao, ZHENG Zhenhua; Formal analysis: LI Qing, LI Dan, YUAN Yixiao; Software: LI Dan; Writing - original draft preparation: LI Dan, WANG Jinfeng; Writing - review and editing: WANG Sheng; Supervision: WANG Sheng; Project administration: WANG Sheng; Funding acquisition: LI Qing, WANG Sheng, WANG Jinfeng; Resources: ZHENG Zhenhua. All authors approved the manuscript.

References

Bai R H, Wang X Z, Li J W, et al. 2024. The impact of vegetation reconstruction on soil erosion in the Loess Plateau. Journal of

Environmental Management, 363: 121382, doi: 10.1016/J.JENVMAN.2024.121382.
Cerretelli S, Castellanos E, Mollinedo S G, et al. 2023. A scenario modelling approach to assess management impacts on soil erosion in coffee systems in Central America. Catena, 228: 107182, doi: 10.1016/j.catena.2023.107182.
Chen L D, Wei W, Fu B J, et al. 2007. Soil and water conservation on the Loess Plateau in China: Review and perspective. Progress in Physical Geography: Earth and Environment, 31(4): 389–403.
Chen Y L, Bai L C, Jiao J Y, et al. 2023. Recognition of suitable small watersheds for check dam construction on the Loess Plateau. Land Degradation & Development, 14: 4441–4455.
Cui L H, Shen Z, Liu Y X, et al. 2023. Identification of driving forces for windbreak and sand fixation services in semiarid and arid areas: A case of Inner Mongolia, China. Progress in Physical Geography: Earth and Environment, 47(1): 32–49.
Cui Y S, Pan C Z, Liu C L, et al. 2020. Spatiotemporal variation and tendency analysis on rainfall erosivity in the Loess Plateau of China. Hydrology Research, 51(5): 1048–1062.
Ed-daoudy L, Lahmam N, Benmansour M, et al. 2023. Hydric erosion rates in Raouz watershed, Morocco: RUSLE, GIS, and remote sensing. Remote Sensing Applications: Society and Environment, 32: 101056, doi: 10.1016/J.RSASE.2023.101056.
Eyring V, Bony S, Meehl G A, et al. 2016. Overview of the Coupled Model Intercomparison Project Phase 6 (CMIP6) experimental design and organization. Geoscientific Model Development, 9(5): 1937–1958.
Feng Q, Zhao W W, Hu X P, et al. 2020. Trading-off ecosystem services for better ecological restoration: A case study in the Loess Plateau of China. Journal of Cleaner Production, 257: 120469, doi: 10.1016/j.jclepro.2020.120469.
Fu B J. 1989. Soil erosion and its control in the Loess Plateau of China. Soil Use & Management, 5(2): 76–82.
Fu B J, Liu Y, Lv Y H, et al. 2011. Assessing the soil erosion control service of ecosystems change in the Loess Plateau of China, Ecological Complexity, 8(4): 284–293.
Fu B J, Wang S, Liu Y, et al. 2017. Hydrogeomorphic ecosystem responses to natural and anthropogenic changes in the Loess Plateau of China. Annual Review of Earth and Planetary Sciences, 45: 223–243.
Gong G L, Yao L, Ren L X, et al. 2020. Effects of ecological protection and construction projects on the service functions of windbreak and sand fixation in the Beijing-Tianjin sandstorm source area. Bulletin of Soil and Water Conservation, 40(5): 181–188. (in Chinese)
Guan Y B, Yang S T, Wang J, et al. 2023. Effects of varying the spatial configuration and scale of terraces on water and sediment loss based on scenario simulation within the Chinese Loess Plateau. Science of the Total Environment, 880: 163182, doi: 10.1016/J.SCITOTENV.2023.163182.
Guo X X, Du M, Gao P, et al. 2024. Response of runoff-sediment processes to vegetation restoration patterns under different rainfall regimes on the Loess Plateau. Catena, 234: 107647, doi: 10.1016/j.catena.2023.107647.
Han Y, Zhao W W, Ding J Y, et al. 2023. Soil erodibility for water and wind erosion and its relationship to vegetation and soil properties in China's drylands. Science of the Total Environment, 903: 166639, doi: 10.1016/j.scitotenv.2023.166639.
Huang M D, Xiao Y, Qin K Y, et al. 2022. Spatio-temporal changes and driving factors of windbreak and sand fixation services in Hunshandak region from 1980 to 2018. Acta Ecologica Sinica, 42(18): 7612–7629. (in Chinese)
Huang Y T, Wu J Y. 2023. Spatial and temporal driving mechanisms of ecosystem service trade-off/synergy in national key urban agglomerations: A case study of the Yangtze River Delta urban agglomeration in China. Ecological Indicators, 154: 110800, doi: 10.1016/j.ecolind.2023.110800.
Jia X X, Shao M A, Zhu Y J, et al. 2017. Soil moisture decline due to afforestation across the Loess Plateau, China. Journal of Hydrology, 546: 113–122.
Jiang C, Wang F, Zhang H Y, et al. 2016. Quantifying changes in multiple ecosystem services during 2000–2012 on the Loess Plateau, China, as a result of climate variability and ecological restoration, Ecological Engineering, 97: 258–271.
Jiang C, Zhang H Y, Zhang Z D, et al. 2019. Model-based assessment soil loss by wind and water erosion in China's Loess Plateau: Dynamic change, conservation effectiveness, and strategies for sustainable restoration. Global and Planetary Change, 172: 396–413.
Jin F M, Yang W C, Fu J X, et al. 2021. Effects of vegetation and climate on the changes of soil erosion in the Loess Plateau of China. Science of the Total Environment, 773: 145514, 10.1016/j.scitotenv.2021.145514.
Jodhani K H, Patel D, Madhavan N, et al. 2023. Soil erosion assessment by RUSLE, Google Earth Engine, and geospatial techniques over Rel River Watershed, Gujarat, India. Water Conservation Science and Engineering, 8(1): 49, doi: 10.1007/s41101-023-00223-x.
Li D J, Xu D Y. 2019. Sand fixation function response to climate change and land use in northern China from 1981 to 2015. Aeolian Research, 40: 23–33.
Li P F, Chen J N, Zhao G J, et al. 2022. Determining the drivers and rates of soil erosion on the Loess Plateau since 1901. Science of the Total Environment, 823: 153674, doi: 10.1016/j.scitotenv.2022.153674.

Li Q, Kou X M, Niu L, et al. 2023. Spatiotemporal variations and its driving factors of soil conservation services in the Three Gorges Reservoir area in China. Frontiers in Environmental Science, 11: 12169, doi: 10.3389/fenvs.2023.12169.

Li X P, Xiao P Q, Hao S L, et al. 2024. Rainfall erosivity characteristics during 1961–2100 in the Loess Plateau, China. Remote Sensing, 16(4): 661, doi: 10.3390/rs16040661.

Li Y H, Gao Z L. 2011. The Loess Plateau area, the characteristics of soil and water loss, damages and management. Ecological Environment, 8: 148–153. (in Chinese)

Li Z G, Zou X Y, Cheng H. 2013. Method of wind erosion sampling survey in China. Science of Soil and Water Conservation, 11: 17–21. (in Chinese)

Liu P, Zhao X N, Gao X D, et al. 2022. Characteristics of extreme temperature variation in the Loess Plateau and its correlation with average temperature. Journal of Applied Ecology, 33(7): 1975–1982. (in Chinese)

Liu Y F, Liu Y, Shi Z H, et al. 2020. Effectiveness of re-vegetated forest and grassland on soil erosion control in the semi-arid Loess Plateau. Catena, 195: 104787, doi: 10.1016/j.catena.2020.104787.

Lu S, Hu Z Y, Fu C W, et al. 2022. Analysis of summer extreme precipitation and its causes in Loess Plateau. Plateau Meteorology, 41(1): 241–254. (in Chinese)

Malathy J, Bhaskar D. 2023. Land use land cover (LULC) dynamics by CA-ANN and CA-Markov Model Approaches: A case study of Ranipet Town, India. Nature Environment and Pollution Technology, 22(3): 1251–1265.

Mu X M, Li P F, Liu B T, et al. 2022. Spatial-temporal development and driving mechanisms of erosion on the Chinese Loess Plateau between 1901 and 2016. Yellow River, 44(9): 36–45. (in Chinese)

Oldeman L, Engelen V, Pulles J. 1990. The extent of human induced soil degradation. In: Oldeman L R, Hakkeling R T A, Sombroek W G. World Map of the Status of Human-induced Soil Degradation: An Explanatory Note (2nd ed.). Wageningen: International Soil Reference and Information Centre.

Pang Y J, Wu B, Jia X H, et al. 2022. Wind-proof and sand-fixing effects of *Artemisia ordosica* with different coverages in the Mu Us Sandy Land, northern China. Journal of Arid Land, 14(8): 877–893.

Ren Y L, Zhang J P, Li B B, et al. 2023. Projecting extreme climate events in China's Loess Plateau: Multiple RCMs and emission scenarios corrected by a trend-preserving method. Theoretical and Applied Climatology, 151: 739–752.

Sai K. 2022. Evaluation of integrated shelter effects of farmlands shelterbelts of different structure and conservative tillage. PhD Dissertation. Beijing: Beijing Forestry University. (in Chinese)

Shen Y P, Zhang C L, Wang X S, et al. 2018. Statistical characteristics of wind erosion events in the erosion area of Northern China. Catena, 167: 399–410.

Shi H, Shao M G. 2000. Soil and water loss from the Loess Plateau in China. Journal of Arid Environments, 45(1): 9–20.

Song R Y, Zhao X F, Jing Y C, et al. 2022. Analysis of ecosystem protection and sustainable development strategies–evidence based on the RWEQ Model on the Loess Plateau, China. Sustainability, 14(18): 11502, doi: 10.3390/su141811502.

Tang K, Zhang P, Zhang H, et al. 1992. Soil erosion disasters on the Loess Plateau: Its prevention and counter measures. In: Shi Y, Embleton C. Geo-hazards and Their Mitigation. Beijing: Science Press, 93–100. (in Chinese)

Tang Q, Xu Y, Bennett S J, et al. 2015. Assessment of soil erosion using RUSLE and GIS: A case study of the Yangou watershed in the Loess Plateau, China. Environmental Earth Sciences, 73: 1715–1724.

UNCCD (United Nation Convention to Combat Desertification). 2022. Chronic land degradation: UN offers stark warnings and practical remedies in global land outlook. [2023-04-27]. https://www.unccd.int/news-stories/press-releases/chronic-land-degradation-un-offers-stark-warnings-and-practical.

Wang J F, Liu X L, Li Q, et al. 2023a. Spatio-temporal differentiation and driving factors of windbreak and sand fixation services in wind erosion area of the northern Loess Plateau. Journal of Desert Research, 43(4): 220–230. (in Chinese)

Wang M W, Wen Y X, Yan D H, et al. 2023b. Assessment of future trend of extreme climate events in the Yellow River Basin. Yellow River, 45(2): 33–37. (in Chinese)

Wang S, Xu M F, Li Q, et al. 2023c. Analysis on trend evolution and driving factors of soil protection services in eastern sandy region of China. Ecological Indicators, 154: 110816, doi: 10.1016/j.ecolind.2023.110816.

Wang X F, Xiao F Y, Feng X M, et al. 2018. Soil conservation on the Loess Plateau and the regional effect: Impact of the 'Grain for Green' Project. Earth and Environmental Science Transactions of the Royal Society of Edinburgh, 109(3–4): 461–471.

Wen X, Zhen L. 2020. Soil erosion control practices in the Chinese Loess Plateau: A systematic review. Environmental Development, 34: 100493, doi: 10.1016/j.envdev.2019.100493.

Williams J R, Jones C A, Dyke P T. 1984. A modeling approach to determining the relationship between erosion and soil productivity. Transactions of the ASAE, 27(1): 129–144.

Wischmeier W H, Johnson C B, Cross B. 1971. Soil erodibility nomograph for farmland and construction sites. Journal of Soils and Water Conservation, 26(5): 189–193.

Wu J, Shi Y, Xu Y, 2020. Evaluation and projection of surface wind speed over China based on CMIP6 GCMs. Journal of Geophysical Research: Atmospheres, 125(22): e2020JD0336113, doi: 10.1029/2020JD033611.

Wu J F, Nunes J P, Baartman J E M, et al. 2023. Disentangling the impacts of meteorological variability and human induced changes on hydrological responses and erosion in a hilly-gully watershed of the Chinese Loess Plateau. Catena, 233: 107478, doi: 10.1016/j.catena.2023.107478.

Wu T G, Yu M K, Wang G, et al. 2013. Effects of stand structure on wind speed reduction in a *Metasequoia glyptostroboides* shelterbelt. Agroforestry Systems, 87: 251–257.

Xi J, Zhao X, Wang X, et al. 2017. Assessing the impact of land use change on soil erosion on the Loess Plateau of China from the end of the 1980s to 2010. Journal of Soil and Water Conservation, 72(5): 452–462.

Xia L, Song X Y, Fu N, et al. 2017. Impacts of precipitation variation and soil and water conservation measures on runoff and sediment yield in the Loess Plateau Gully Region, China. Journal of Mountain Science, 14(10): 2028–2041.

Xiao W W, An B. 2023. Spatial-temporal variation of wind speed in the Loess Plateau during 1960–2017. Research of Soil and Water Conservation, 30(4): 103–109. (in Chinese)

Yang W Q, Zhang G F, Yang H M, et al. 2023. Review and prospect of soil compound erosion. Journal of Arid Land, 15(9): 1007–1022.

Yang Y F, Wang B, Wang G L, et al. 2019. Ecological regionalization and overview of the Loess Plateau. Acta Ecologica Sinica, 39(20): 7389–7397. (in Chinese)

Zhang H P, Song H Q, Wang X W, et al. 2023a. Effect of agricultural soil wind erosion on urban $PM_{2.5}$ concentrations simulated by WRF-Chem and WEPS: A case study in Kaifeng, China. Chemosphere, 323: 138250, doi: 10.1016/j.chemosphere.2023.138250.

Zhang Y X, Li P, Xu G C, et al. 2023b. Temporal and spatial variation characteristics of extreme precipitation on the Loess Plateau of China facing the precipitation process. Journal of Arid Land, 15: 439–459.

Zhao J, Feng X M, Deng L, et al. 2020. Quantifying the effects of vegetation restorations on the soil erosion export and nutrient loss on the Loess Plateau. Frontiers Plant Science, 11: 573126, doi: 10.3389/fpls.2020.573126.

Zhao X M, Cheng H, Jiang N, et al. 2023. Spatiotemporal pattern and evolution of wind erosion in Beijing-Tianjin sand-source soil. Chinese Science Bulletin, 68(2): 238–253. (in Chinese)

Zhou Y G, Wu Z F, Hu R N, et al. 2020. Characteristics of soil wind erosion in newly reclaimed land in Mu Us Sandy Land. Transactions of the Chinese Society of Agricultural Engineering, 36(1): 138–147. (in Chinese)

Zhu J J, Jiang F Q, Fang Z P, et al. 2003. Optimization of spatial arrangements and patterns for shelterbelts or windbreaks. Chinese Journal of Applied Ecology, 14(8): 1205–1212. (in Chinese)

Zhu R P, Yu Y, Zhao J C, et al. 2023. Evaluating the applicability of the water erosion prediction project (WEPP) model to runoff and soil loss of sandstone reliefs in the Loess Plateau, China. International Soil and Water Conservation Research, 11(2): 240–250.

Zou H J, Liu G, Zhang Q, et al. 2024. Investigating the effects of water and wind erosion on different hillslope aspects on the Loess Plateau of China by using ^{137}Cs. Catena, 238: 107879, doi: 10.1016/j.catena.2024.107879.

Appendix

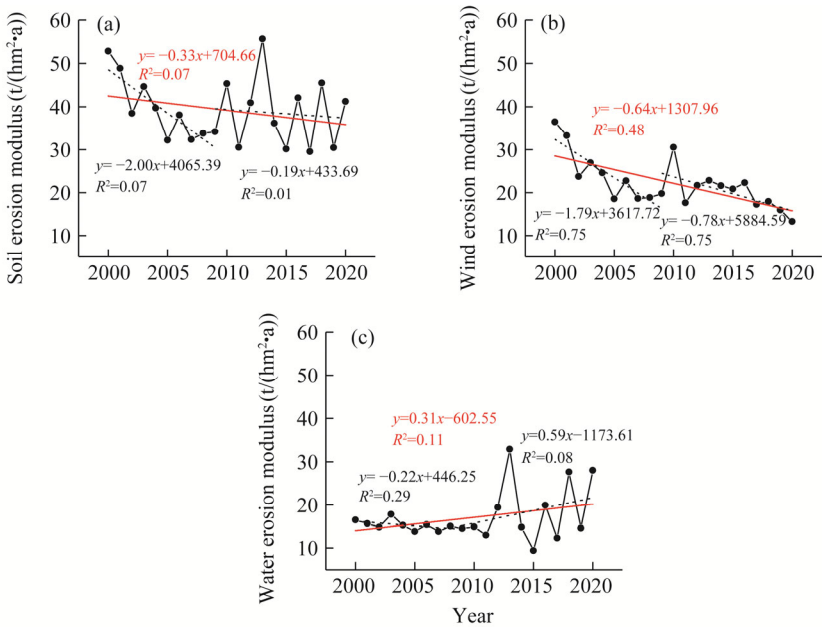

Fig. S1 Inter-annual variations of soil erosion modulus (a), wind erosion modulus (b), and water erosion modulus (c). Red lines and functions represent the overall trend lines and trend functions for each parameter during 2000–2020, and black dashed lines and functions represent the overall trend lines for each parameter during 2000–2009 and 2010–2020.

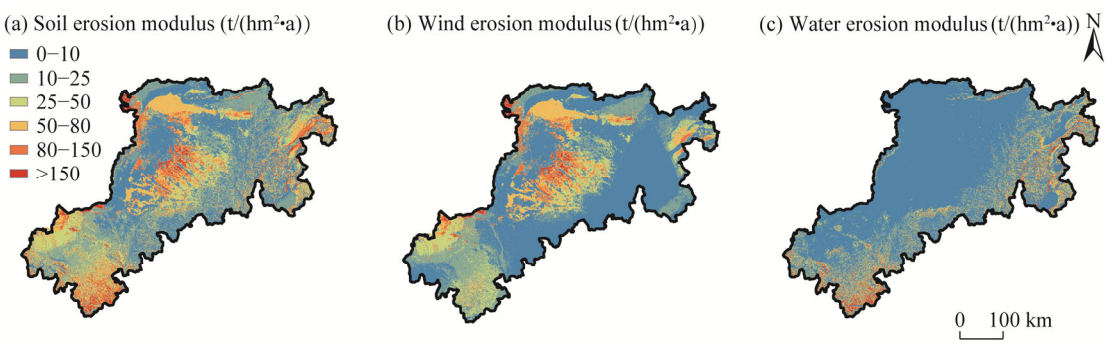

Fig. S2 Spatial distribution patterns of soil erosion modulus (a), wind erosion modulus (b), and water erosion modulus (c)